AD_____

Award Number: DAMD17-03-1-0119

TITLE: Ultrasound Activated Contrast Imaging for Prostate Cancer Detection

PRINCIPAL INVESTIGATOR: Flemming Forsberg, Ph.D.

CONTRACTING ORGANIZATION: Thomas Jefferson University
Philadelphia, PA 19107

REPORT DATE: March 2004

TYPE OF REPORT: Annual

PREPARED FOR: U.S. Army Medical Research and Materiel Command
Fort Detrick, Maryland 21702-5012

DISTRIBUTION STATEMENT: Approved for public release;
Distribution Unlimited

REPORT DOCUMENTATION PAGE

Form Approved
OMB No. 074-0188

1. AGENCY USE ONLY (Leave blank)	2. REPORT DATE	3. REPORT TYPE AND DATES COVERED
	March 2004	Annual (March 1, 2003 - February 28, 2004)

4. TITLE AND SUBTITLE

Ultrasound Activated Contrast Imaging for Prostate Cancer Detection

5. FUNDING NUMBERS

DAMD17-03-1-0119

6. AUTHOR(S)

Flemming Forsberg, Ph.D.

7. PERFORMING ORGANIZATION NAME(S) AND ADDRESS(ES)

Thomas Jefferson University
Philadelphia, PA 19107

E-MAIL:
Flemming.Forsberg@jefferson.edu

8. PERFORMING ORGANIZATION REPORT NUMBER

9. SPONSORING / MONITORING AGENCY NAME(S) AND ADDRESS(ES)

U.S. Army Medical Research and
Materiel Command
Fort Detrick, Maryland 21702-5012

10. SPONSORING / MONITORING AGENCY REPORT NUMBER

11. SUPPLEMENTARY NOTES

12a. DISTRIBUTION / AVAILABILITY STATEMENT

Approved for public release; distribution unlimited

12b. DISTRIBUTION CODE

13. ABSTRACT ***(Maximum 200 Words)***

The diagnosis of prostate cancer is currently based on elevated PSA levels or abnormal digital rectal examination confirmed with needle biopsy of the prostate. However, for most screening populations, the frequency of positive biopsy findings is as low as 25%. Therefore, an accurate, noninvasive diagnostic imaging examination of the prostate is needed as a replacement of or an alternative to biopsy. Hence, the current project proposes to develop a novel ultrasound contrast imaging technique (called EEI) for better visualization of the microvessels, which are characteristic of the neovasculature associated with prostate cancer.

To date, a pulse-echo system was built to perform in vitro EEI measurements and initial experiments were conducted with 4 contrast agents. Up to 10 dB of enhancement was measured at 37°C with Optison. Higher frequency detection pulses are currently being evaluated. A new zero-thickness interface model was developed to describe the encapsulation of microbubble contrast agents. While the model was fitted based on linear measurements, the model predictions were compared to measured nonlinear subharmonic signals. The current model shows a much better match with the experimental data at frequencies of 3.0 and 4.4MHz than other models. The dual pulse imaging mode associated with EEI is currently being modeled.

14. SUBJECT TERMS	15. NUMBER OF PAGES
Prostate Cancer, Ultrasound Imaging, Ultrasound Contrast Agent	15
	16. PRICE CODE

17. SECURITY CLASSIFICATION OF REPORT	18. SECURITY CLASSIFICATION OF THIS PAGE	19. SECURITY CLASSIFICATION OF ABSTRACT	20. LIMITATION OF ABSTRACT
Unclassified	Unclassified	Unclassified	Unlimited

3. TABLE OF CONTENTS

4. INTRODUCTION

The diagnosis of prostate cancer is currently based on an elevated prostate-specific antigen (PSA) level or abnormal digital rectal examination findings confirmed by needle biopsy of the prostate. It is estimated that the number of men subjected to biopsy of the prostate in the U.S. in 2001 exceeded 600,000 [1]. Unfortunately, the frequency of positive biopsy findings, for most screening populations, was as low as one in three to one in four. Therefore, an accurate, noninvasive diagnostic imaging examination of the prostate is needed to reduce the number of biopsies or even to replace biopsy.

A sextant biopsy of the prostate, consisting of the acquisition of six biopsy cores, can miss clinically detectable prostate caner in up to 34% of men. Among patients with an elevated PSA level and a negative initial sextant biopsy finding, repeat biopsy demonstrates the presence of malignancy in approximately 20%-30% [2]. However, each additional biopsy is associated with a small incremental risk of hemorrhage and infection. Thus, an accurate, noninvasive imaging technique is useful for targeted biopsy guidance in order to reduce the number of biopsies in each prostate.

The sensitivity and specificity of ultrasound imaging can be improved by intravenous injection of vascular contrast agents consisting of encapsulated gas microbubbles [3]. Due to encapsulation, these agents are stable enough to pass through the pulmonary circulation and flow in intravascular space for at least several minutes. However, encapsulation imposes severe restrictions on the oscillations of contrast bubbles. Based on de Jong's numerical model [4], our calculations indicate that the incident acoustic pressure amplitude for an albumin-encapsulated Abunex® bubble is 18 times greater than that for a free bubble if the two bubbles oscillate with the same relative amplitude at their resonant frequency of 2 MHz. Hence, scattering can be greatly enhanced if encapsulated bubbles become free bubbles. According to the Rayleigh's approximation, the fundamental scattering cross-section of an air bubble is more than 200 times (47 dB) greater than that for an Abunex bubble of the same size. Furthermore, the enhancement in second or sub- harmonic scattering cross-section must be even much greater because encapsulation dampens nonlinear oscillations to a much greater degree.

Unlike current ultrasound imaging modalities employing only an imaging field, the proposed technique utilizes two acoustic fields: the activation field for intermittently activating contrast bubbles and the imaging field, applied shortly afterwards, for acquiring harmonic or subharmonic images with significantly enhanced scattering signals from activated contrast bubbles. This new imaging mode is referred to as Excitation Enhanced Imaging (EEI) [5]. Based on previous work on ultrasound-induced contrast scattering enhancement and contrast-assisted ultrasonographic detection of human and canine prostate cancer, the hypotheses of this study are: (1) contrast microbubbles can be ultrasonically activated to achieve marked backscattering enhancement, and (2) the detection of prostate cancer can be improved using the proposed ultrasonographic technique. It is well known that a free bubble resonating at the insonation frequency is the optimal acoustic scatterer. Hence, the activation field will consist of a release pulse for

effectively releasing free bubbles from encapsulated contrast bubbles and an excitation pulse for shifting the free bubbles to the resonance size corresponding to a pre-selected imaging frequency.

5. BODY

It is the central hypothesis of this study that contrast microbubbles can be activated and backscattering enhanced markedly. The activation field will produce the optimal acoustic scatterers, i.e., free bubbles resonant around a pre-selected imaging frequency. In the proposed study, both the modeling and measurement will help us to determine optimal contrast agents and develop optimal activation pulse sequences enhancing backscattered second and sub-harmonic signals by a factor of 2 to 16, i.e., by 6 to 24 dB. The other hypothesis of this study is that prostate cancer can be detected using the proposed ultrasonographic technique. This hypothesis will be tested using an established canine prostate tumor model. The specific tasks of the project (as presented in the original Statement of Work) can be found in Appendix I.

First an outline of the methods applied will be given followed by a presentation of the results to date. Finally, the conclusions and future directions of the research will be discussed.

5.1 Methods

Contrast microbubble modeling

The interface of an encapsulated contrast microbubble gives rise to interfacial forces that are modeled by rheology. We have adopted a Newtonian rheology, i.e., only viscous interfacial stresses are considered (see [6] for details). Assuming spherical symmetry (for a micron size bubble in a pressure field of 1 MHz, the radius to wavelength ratio is too small, $\sim 10^{-3}$, to experience substantial shape deformation except for extreme cases of microbubble breakup), the normal (r-component) stress boundary condition at the bubble radius ($r = R$), given by:

$$p(r=R,t) = P_G - 4\mu\frac{\dot{R}}{R} - \frac{4\kappa^s\dot{R}}{R^2} - \frac{2\gamma}{R}. \qquad (1)$$

$p(r=R,t)$ is the pressure in the liquid immediately outside of the bubble, P_G is the uniform gas pressure inside the bubble (Fig 1b), μ the liquid viscosity, κ^s and γ are interfacial dilatational viscosity and surface tension respectively. $\dot{R}$ is the bubble wall velocity while R is the instantaneous bubble radius. The gas pressure inside the bubble is assumed to vary with bubble volume polytropically with k as the polytropic exponent as follows:

$$P_G R^{3k} = P_{G0} R_0^{\,3k}. \qquad (2)$$

P_{G0} is the gas pressure and $R=R_0$ at time $t=0$. Given the boundary condition of eqn. (1) for the liquid-gas system, we obtain the modified Rayleigh-Plesset type equation (for details see [6]):

$$\rho(R\ddot{R} + \frac{3}{2}\dot{R}^2) = P_{G0}\left(\frac{R_0}{R}\right)^{3k} - 4\mu\frac{\dot{R}}{R} - \frac{2\gamma}{R} - \frac{4\kappa^s\dot{R}}{R^2} - P_0 + P_A\sin\omega t, \qquad (3)$$

where, P_0 is the liquid hydrostatic pressure, $\omega=2\pi f$ with f being the driving frequency and P_A is the acoustic pressure amplitude. At $t=0$, $R(t=0)=R_0$, and $\dot{R}(t=0)=0$. Eqn (3) together with these initial conditions describes the bubble dynamics. Note that the third and the fourth terms in the right-hand-side contain the effects of the interface. This model represents the completion of Task 1b as outlined in the original SOW (see the Appendix).

The acoustic pressure $P_s(t)$ scattered by a bubble is (in [7], p.83):

$$P_s(r,t)=\rho\frac{R}{r}\left(2\dot{R}^2+R\ddot{R}\right) \tag{4}$$

Subharmonic component of the scattered signal is determined by transforming this time-domain expression into frequency domain (i.e., $P_s(\omega)$). For comparison, we have also computed similar results for the Church's shell model [8] using the formulation presented by Hoff et al [9] (eqn. (6) in their paper). This model is hereafter referred to as the Church-Hoff model.

In Vitro experiments

A system was built to perform EEI and measure the enhancement of scattered signals from contrast microbubbles in a water bath with three single-element spherically-focused transducers (Staveley, East Hartford, CT, USA), as shown in Figure 1. An excitation transducer (1.1 or 2.1 MHz) with a diameter of 2.5 cm and a focal length of 5.0 cm was used for conditioning microbubbles and a pair of small broadband imaging transducers (with center frequencies of 2-10 MHz), for detecting these microbubbles before and after conditioning. Both imaging transducers had a diameter of 1.2 cm and a focal length around 2.6 cm. The three transducers were placed confocally and the positioning was guided with a 0.2 mm miniature needle hydrophone (Precision Acoustics, Dorchester, UK). The advantage of this measurement system is its high spatial resolution. This is because scattered signals only come from the microbubbles in the small overlapping confocal region of the transmit and receive transducers. The size of the confocal region is determined by the beam diameter (less than 2 mm) at the focus of each transducer.

The excitation transducer was driven by a programmable arbitrary function generator (LW420; LeCroy, Chestnut Ridge, NY, USA) through a 500 W power amplifier (A-500; ENI, Rochester, NY, USA). One imaging transducer was used to transmit imaging pulses produced by a programmable function generator (8116A; Hewlett Packard, Santa Clara, CA, USA) and a broadband power amplifier (325LA; ENI) and another was employed to receive signals scattered from the contrast microbubbles. The scattered signals were amplified with a low-noise RF amplifier (5052 PR; Parametrics, Waltham, MA, USA) and then acquired using a digital oscilloscope (9350AM; LeCroy, Chestnut Ridge, NY, USA). A time modulus (AV-1023-C; Avtech Electosystems, Ogdensberg, NY, USA) was used to synchronize the delay between the conditioning and imaging pulses. The command delivery to the function generators and the data transfer from the digital oscilloscope were controlled by LabView® (National Instruments, Austin, TX, USA). The acoustic pressure amplitudes were calibrated using a 0.5 mm diameter needle hydrophone (Precision Acoustics Ltd, Dorchester, UK) with an excellent sensitivity over 1 to 20 MHz. This setup represents the completion of Task 1a.

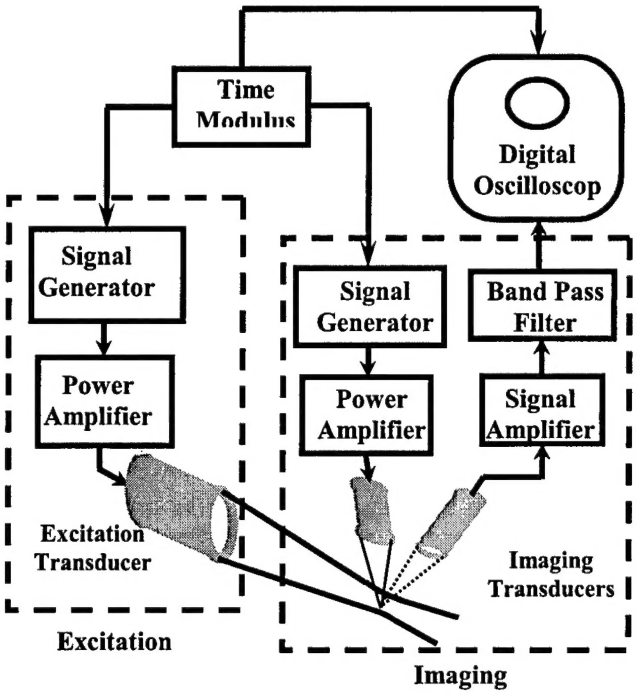

Figure 1. *Experimental set-up for EEI enhancement measurement. An excitation transducer was used to condition contrast microbubbles and a pair of broadband transducers (one for transmission and another for reception, perpendicular to each other and to the excitation transducer) were employed to detect the conditioned microbubbles.*

Four different types of contrast agents were tested: a) Sonazoid® (Amersham Health, Oslo, Norway), a lipid-coated contrast agent containing a PFC gas; b) Optison® (Mallinckrodt, St. Louis, MO), an albumin-encapsulated agent filled with perfluorobutane; c) Definity® (Bristol-Myers Squibb, N. Billerica, MA), consisting of PFC-filled microbubbles with a lipid bi-layer shell; and d) QFX (Nanfang Hospital, Guangzhou, China), made up of PFC microbubbles stabilized with albumin coating. During the experiments, contrast agents were diluted in water (e.g., around 20 μl of reconstituted Sonazoid per liter of water) and a magnetic stirrer was used to maintain mixture. Excitation amplitudes of 0.4, 0.8, 1.2 and 1.6 MPa were investigated along with excitation pulse lengths of 2, 4, 16 and 128 cycles operating at pulse repetition frequencies (PRFs) of 1, 2, 10 and 20 Hz. Inter-pulse delays from 10 to 750 μs were studied.

In vitro experiments were conducted at ambient temperature (22° C) and physiological temperature (37° C). For each enhancement measurement, spectra of scattered imaging signals from unconditioned and conditioned contrast microbubbles were acquired. The average spectrum for regular contrast microbubbles (before conditioning) was obtained at a given PRF based on a sequence of 64 scattered signals from transmit imaging pulses. The same imaging pulse was transmitted with a given delay after each condition pulse for 64 times (at the same PRF), so that the averaged spectrum for the conditioned microbubbles was obtained.

5.2 Results and Discussion

To examine the validity of our novel simulation model, we used the Rayleigh-Plesset equation of eqn (3) with parameters κ^s = 0.01 msP and γ = 0.6 N/m to simulate the dynamic behavior of microbubbles. The far-field nonlinear scattering was computed from the time evolution of bubble radius using eqn. (4). After performing an FFT, the subharmonic response was compared to experimental observations (for details on the experimental data acquisition see [10]). The simulation is scaled to match the experimental data for the lowest pressure level. Note that the model parameters were determined using the linearized equations valid only for small oscillations. The underlying assumption is that a Newtonian rheology holds for the interface, and the determined material properties remain constant in a range of magnitude of oscillation (they may change for too large an oscillation, e.g. shear rate dependent interface viscosity and interfacial tension).

Figure 2 shows subharmonic emission for Sonazoid at several frequencies along with the model prediction. For comparison, the predictions from Church-Hoff model have also been included. The corresponding root-mean-square-error (RMSE) for the estimation using the two models is presented in Table 1. At frequencies of 3 and 4.4 MHz, the new model predicts better than the Church-Hoff model, whereas at frequencies of 2 and 6 MHz, the performance of two models are comparable with the Church-Hoff model performing slightly better. These results have been submitted to a peer-reviewed journal for publication [11].

A pulse-echo system was built (as outlined in Fig. 1) to perform EEI. The change in scattered signal strength before and after the excitation pulse (i.e., the enhancement obtained with EEI relative to standard contrast imaging) was measured under different acoustic conditions. In Figure 3a, an example based on measurements with Sonazoid at 22° C is shown. EEI induces scattering enhancement with a maximum of approximately 10 dB around 3.0 and 6.0 MHz (the fundamental and second harmonic frequencies) for Sonazoid microbubbles conditioned with 1.2 MPa excitation pulses (1.1 MHz and 16 cycles) at 2 Hz PRF. Imaging pulses (36 cycles, 3.0 MHz and 0.1 MPa) were transmitted, with a delay of 100 μs between the conditioning pulse and the detection pulse. However, when the temperature was elevated to the physiological level (i.e., 37° C; Fig. 3b) no enhancement could be observed. Clearly, this means that EEI with Sonazoid would not be beneficial *in vivo*. Similar results were obtained with Definity and QFX.

Table 1: Error in estimating the subharmonic response of Sonazoid using the new model and the Church-Hoff model.

Driving frequency (MHz)	RMSE (%)	
	New Model	Church-Hoff Model
2.0	22.42	19.69
3.0	16.62	26.08
4.4	24.91	40.36
6.0	16.36	12.10

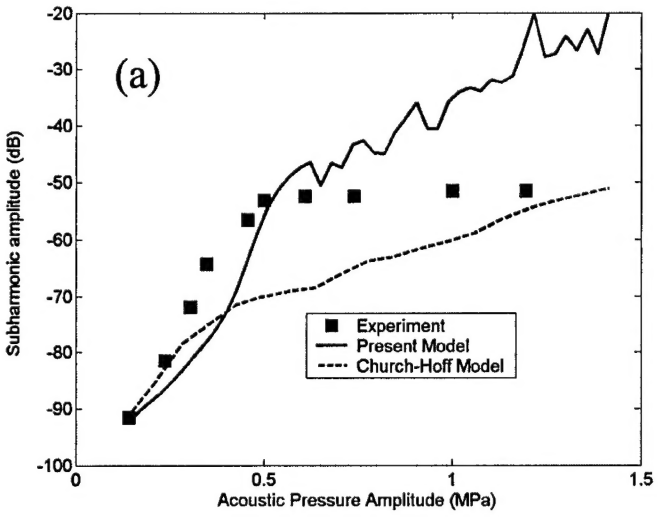
(a)
Subharmonic amplitude (dB)
Acoustic Pressure Amplitude (MPa)
Experiment
Present Model
Church-Hoff Model

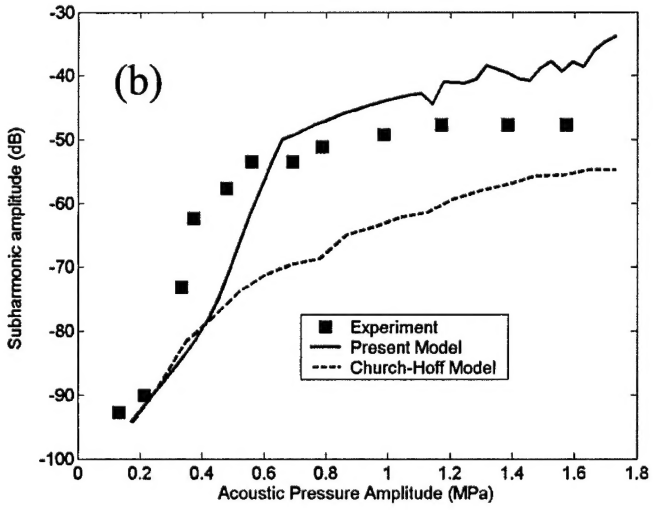
(b)
Subharmonic amplitude (dB)
Acoustic Pressure Amplitude (MPa)
Experiment
Present Model
Church-Hoff Model

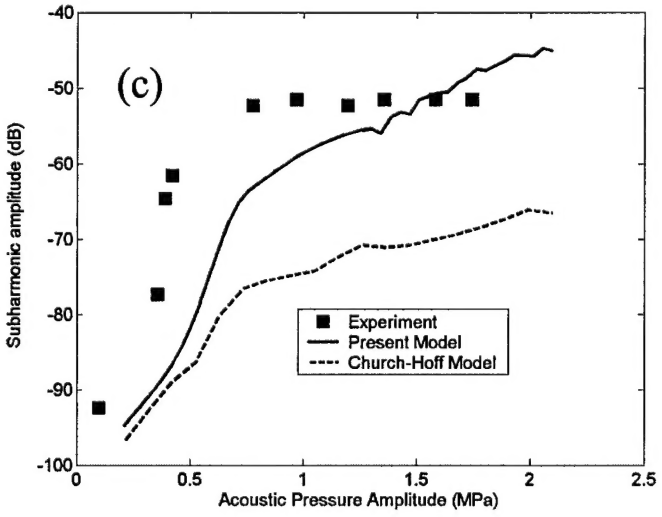
(c)
Subharmonic amplitude (dB)
Acoustic Pressure Amplitude (MPa)
Experiment
Present Model
Church-Hoff Model

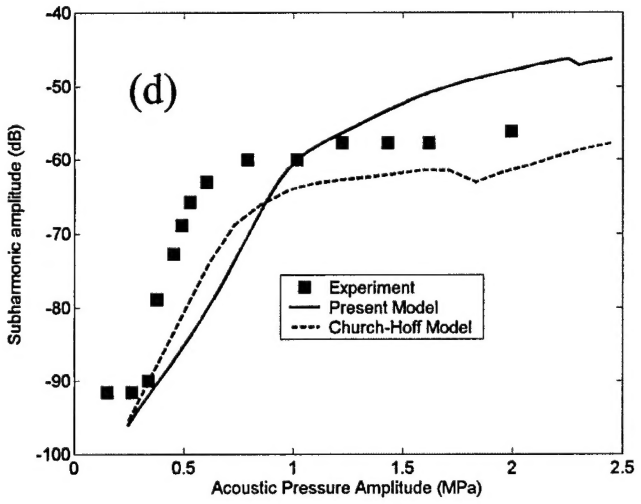

Figure 2. *Predicted and measured subharmonic response at various acoustic pressure amplitudes for Sonazoid. Center frequencies used in these results are as follows: (a) 2.0 MHz, (b) 3.0 MHz, (c) 4.4 MHz and (d) 6.0 MHz.*

However, EEI with Optison (employing the same conditioning and imaging conditions) produced very different results. Figure 4 demonstrates limited enhancement at 22° C, whereas 10 dB of enhancement is seen at 37° C (Fig. 4b); albeit only at the fundamental frequency (of 3.0 MHz). These results show that *in vivo* fundamental EEI with Optison should be feasible. Further experiments are ongoing to study this effect at higher imaging frequencies applicable to prostate cancer imaging.

6. KEY RESEARCH ACCOMPLISHMENTS

- A dual-transducer pulse-echo system was built to perform EEI.
- Initial experiments were conducted with 4 contrast agents.
- Temperature and concentration dependencies were studied.
- Up to 10 dB of enhancement was measured at 37° C for Optison.
- A new zero-thickness interface model was developed to describe the encapsulation of microbubble contrast agents.
- Model predictions were compared with measured nonlinear subharmonic signals (even though the model was fitted using linearized dynamics).

(a)

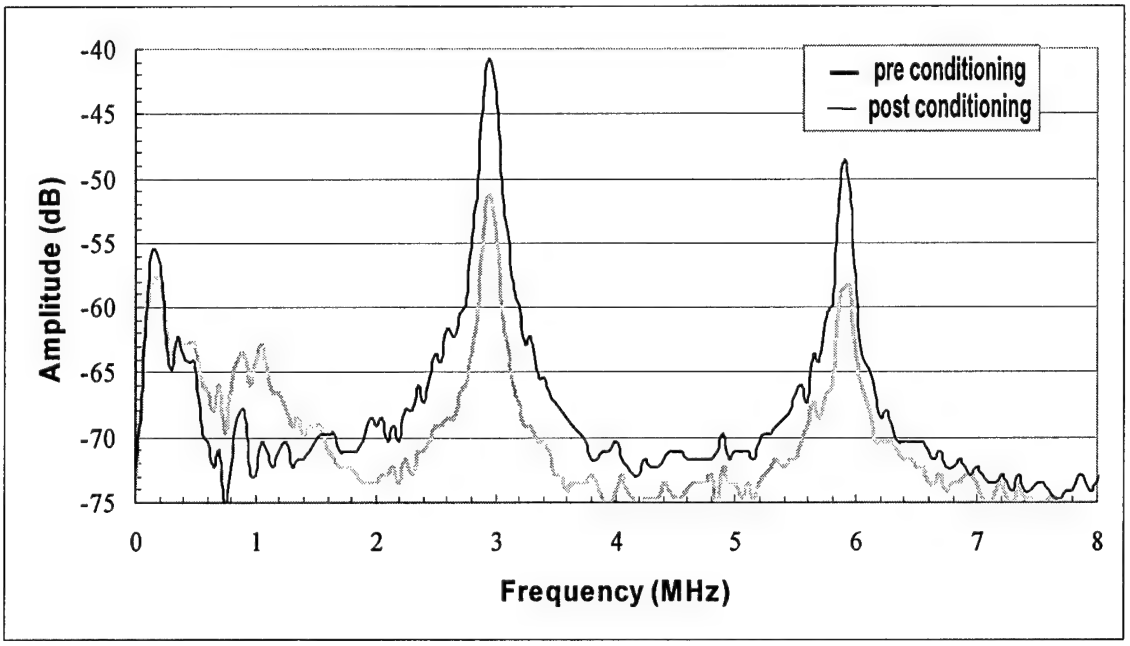

(b)

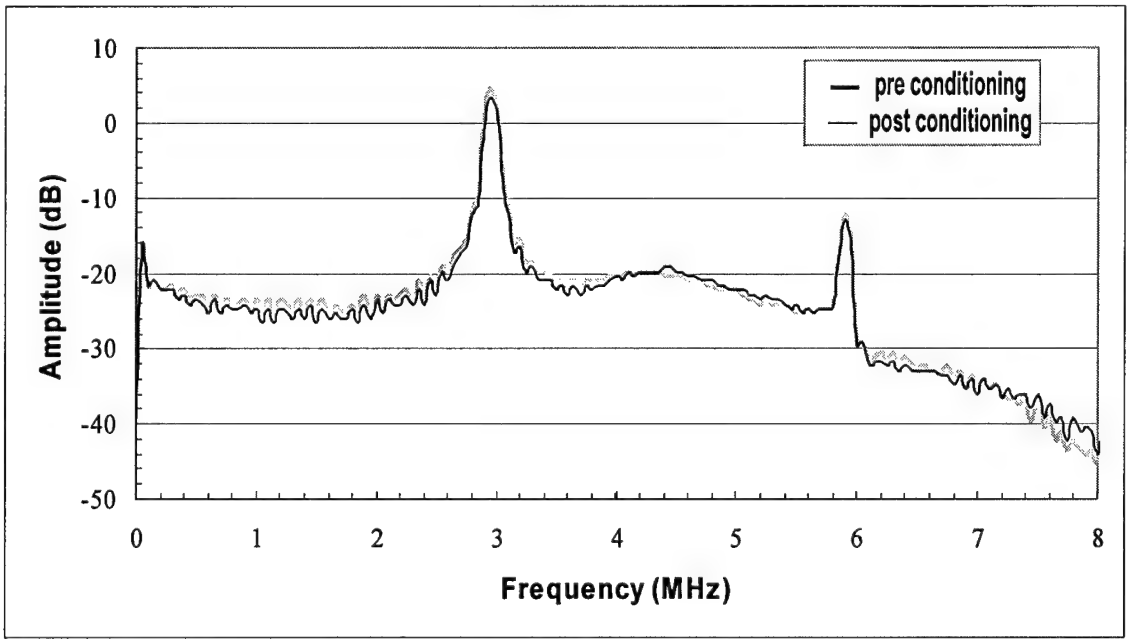

Figure 3. *Measurement of enhancement from Sonazoid in EEI mode using 1.1 MHz excitation at 1.2 MPa, 2 Hz PRF obtained at (a) 22° C and (b) at 37° C. Notice, that no enhancement is seen at the physiological temperature (whereas marked enhancement ~10 dB occurs at room temperature).*

(a)

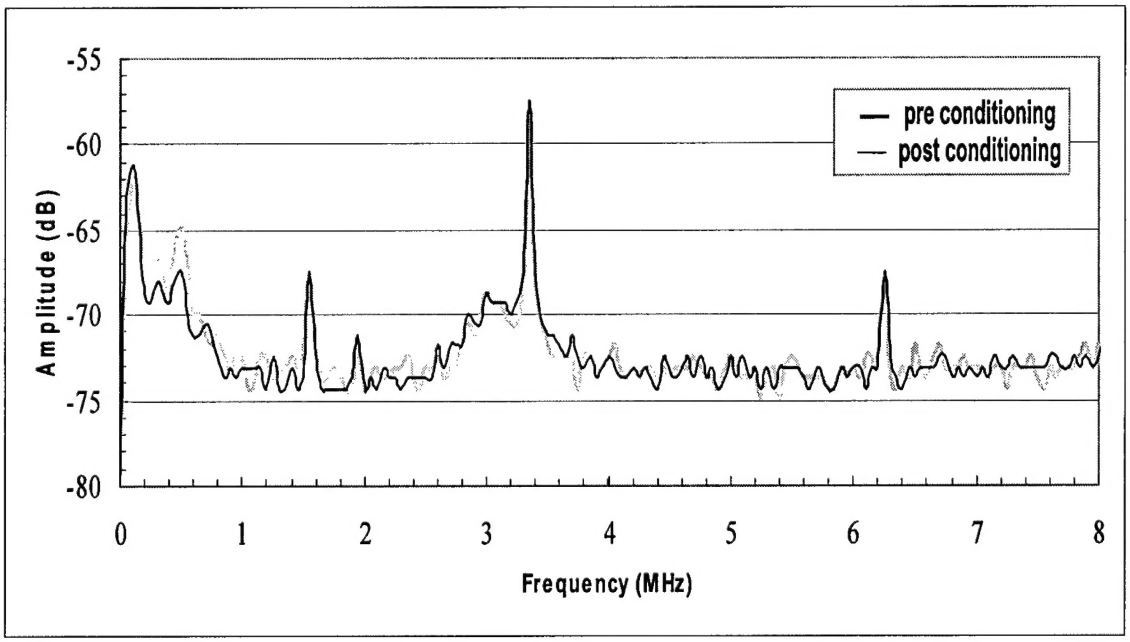

(b)

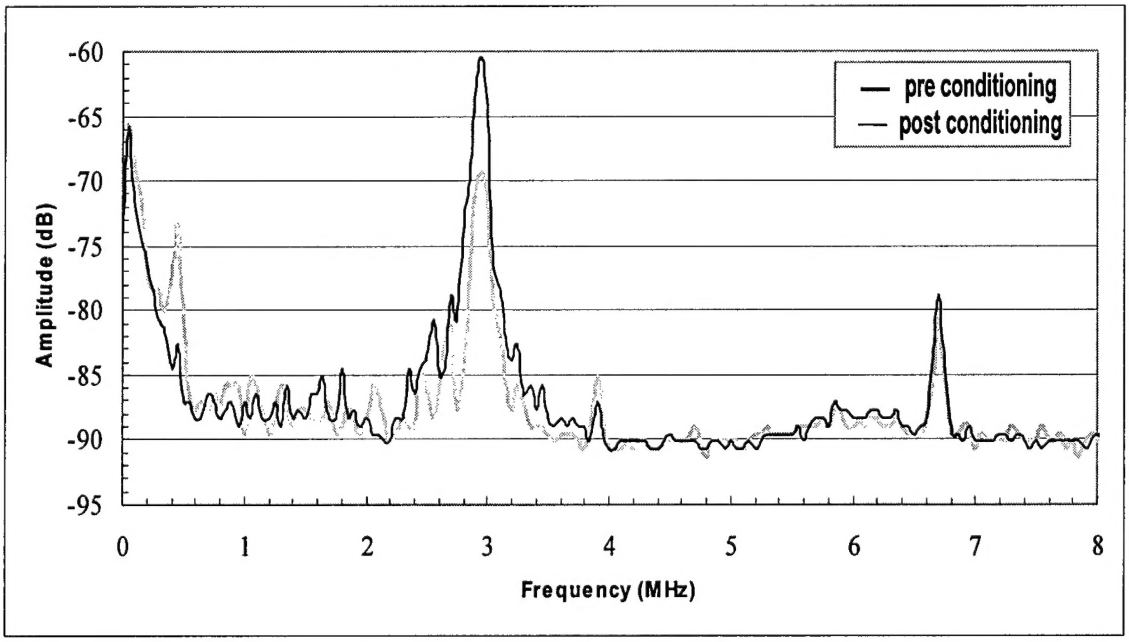

Figure 4. *Measurement of enhancement from Optison in EEI mode using 1.1 MHz excitation at 1.2 MPa, 2 Hz PRF obtained at (a) 22° C and (b) at 37° C. Notice, that no enhancement is seen at room temperature, but at the physiological temperature 10 dB of enhancement is observed at the fundamental frequency.*

7. REPORTABLE OUTCOMES

D. Chatterjee, W. T. Shi, K. Sarkar, F. Forsberg. Characterization of Sonazoid® and its subharmonic response: Model and experiment. Submitted to IEEE Trans Ultrason Ferroelec Freq Control, November, 2003.

February 6 - 7, 2004 — 9th Ultrasound Contrast Research Symposium in Radiology, San Diego, CA, USA.

- On the temperature and concentration dependency of Excitation-Enhanced Imaging.

8. CONCLUSIONS

A pulse-echo system was built to perform in vitro EEI measurements and initial experiments were conducted with 4 contrast agents. Up to 10 dB of enhancement was measured at 37° C with Optison. Higher frequency detection pulses are currently being evaluated.

A new zero-thickness interface model was developed to describe the encapsulation of microbubble contrast agents. While the model was fitted based on linear measurements, the model predictions were compared to measured nonlinear subharmonic signals. The current model shows a much better match with the experimental data at frequencies of 3.0 and 4.4 MHz than other models. The dual pulse imaging mode associated with EEI is currently being modeled.

In summary, tasks 1a and 1b have been completed while tasks 1c and 1d are ongoing. Consequently, the project is reasonably on target according to the original schedule.

9. REFERENCES

1. Halpern EJ, Frauscher F, Forsberg F, Nazarian LN, O'Kane P, Gomella LG. High-frequency Doppler US of the prostate: effect of patient position. *Radiology,* 222:634-639, 2002.
2. Pryor MB, Schellhammer PF. The pursuit of prostate cancer in patients with a rising prostate-specific antigen and multiple negative transrectal ultrasound-guided prostate biopsies. Clin Prostate Cancer, 1:172-176, 2002.
3. Goldberg BB, Raichlen JS, Forsberg F. *Ultrasound Contrast Agents: Basic Principles and Clinical Applications* (2nd Ed). Martin Dunitz Ltd., England, 2001.
4. de Jong N, Cornet R, Lancee CT. Higher harmonics of vibrating gas-filled microspheres. part one: simulations. *Ultrasonics*, 32:447-453, 1994.
5. W. T. Shi, F. Forsberg, R. Bautista, C. Vecchio, R. Bernardi, B. B. Goldberg: Image enhancement by acoustic conditioning of ultrasound contrast agents. *Ultrasound Med Biol*, vol. 30, no. 2, pp. 191 – 198, 2004.
6. Chatterjee D, Sarkar K. A Newtonian rheological model for the interface of microbubble contrast agents. *Ultrasound Med Biol,* 29:1749-1757, 2003.
7. Brennen CE. *Cavitation and Bubble Dynamics*. Oxford University Press, New York, 1995.
8. Church CC. The effects of an elastic solid surface layer on the radial pulsations of gas bubbles. *J. Acoust. Soc. Am.*, 97:1510-1521, 1995.
9. Hoff L, Sontum PC, Hovem JM. Oscillations of polymeric microbubbles: effect of the encapsulating shell. *J. Acoust. Soc. Am.*, 107:2272-2280, 2000.
10. Shi WT, Hoff L, Forsberg F. Subharmonic performance of contrast microbubbles: an experimental and numerical investigation. *Proc IEEE US Symp*, 1908-1911, 2002.
11. Chatterjee D, Shi WT, Sarkar K, Forsberg F. Characterization of Sonazoid® and its subharmonic response: model and experiment. Submitted to *IEEE Trans Ultrason Ferroelec Freq Control*, November, 2003.

Appendix I

The Statement of Work from the original proposal:

Task 1: To investigate activation-induced scattering enhancement at different center frequencies, amplitudes, and shapes (or lengths) of activation pulse sequences (Months 1-18):

a. Construct an *in vitro* experimental system for ultrasonically activating contrast microbubbles and measuring the resulting changes in backscattering (Months 1-2).
b. Design and develop numerical codes for a theoretical model describing the dynamics and instability of ultrasonically activated contrast microbubbles (Months 1-6).
c. Calculate the behavior of individual contrast microbubble and the collective behavior of contrast microbubble populations (Months 6-18).
d. Measure changes in backscattered fundamental, second and sub-harmonic signals before and after activation (Months 3-18).
e. Predict optimal contrast agents for ultrasound-activated contrast imaging according to the numerical simulations (Months 12-18)
f. Select optimal contrast agents for ultrasound-activated contrast imaging. The selection is mainly based on experimental measurements (Months 12-18).
g. Develop activation and imaging strategies, based on both numerical simulations and experimental measurements for the scattering enhancement (Months 12-18).

Task 2: To implement ultrasound-activated contrast imaging (Months 18-24):

a. Produce and evaluate activation-enhanced A-lines in an *in vitro* perfusion phantom using the simple pulse-echo system (Months 18-20).
b. Optimize activation and imaging strategies, based on *in vitro* phantom measurements and simulations with actual parameters of designated transducers (Months 18-24).
c. Modify a state-of-the-art ultrasound imaging system to incorporate the ultrasound-activated contrast imaging modality (Months 21-24).
d. Evaluate the new imaging modality in an *in vitro* perfusion phantom using the modified ultrasound scanner (Months 21-24).

Task 3: To validate the clinical potential of ultrasound-activated contrast imaging using an established canine prostate cancer model (Months 25-32):

a. Create and grow prostate tumors by implanting a Canine Transmissible Venereal Sarcoma (CTVS) cell line into the prostate (Months 25-29).
b. Produce and evaluate activation-enhanced contrast images of canine prostates with CTVS tumors (Months 26-30).
c. Perform pathological evaluations of prostate specimens and quantify the microvessel density with immunohistochemical staining (Months 28-31).
d. Process data and images and write final report (Months 31-32).